

Brain gray matter abnormalities in osteoarthritis pain: a cross-sectional evaluation

Joana Barroso^{a,b,c}, Andrew D. Vigotsky^d, Paulo Branco^c, Ana Mafalda Reis^e, Thomas J. Schnitzer^{b,f,g}, Vasco Galhardo^a, A. Vania Apkarian^{b,c,g,*}

Abstract

The interaction between osteoarthritis (OA) pain and brain properties remains minimally understood, although anatomical and functional neuroimaging studies suggest that OA, similar to other chronic pain conditions, may impact as well as partly be determined by brain properties. Here, we studied brain gray matter (GM) properties in OA patients scheduled to undergo total joint replacement surgery. We tested the hypothesis that brain regional GM volume is distinct between hip OA (HOA) and knee OA (KOA) patients, relative to healthy controls and moreover, that these properties are related to OA pain. Voxel-based morphometry group contrasts showed lower anterior cingulate GM volume only in HOA. When we reoriented the brains (flipped) to examine the hemisphere contralateral to OA pain, precentral GM volume was lower in KOA and HOA, and 5 additional brain regions showed distortions between groups. These GM changes, however, did not reflect clinical parameters. Next, we subdivided the brain into larger regions, approximating Brodmann areas, and performed univariable and machine learning-based multivariable contrasts. The univariable analyses approximated voxel-based morphometry results. Our multivariable model distinguished between KOA and controls, was validated in a KOA hold-out sample, and generalized to HOA. The multivariable model in KOA, but not HOA, was related to neuropathic OA pain. These results were mapped into term space (using Neurosynth), providing a meta-analytic summary of brain anatomical distortions in OA. Our results indicate more subtle cortical anatomical differences in OA than previously reported and also emphasize the interaction between OA pain, namely its neuropathic component, and OA brain anatomy.

Keywords: Osteoarthritis, Chronic pain, Structural brain anomalies, Gray matter volume, VBM

1. Introduction

Osteoarthritis (OA) is the most common form of arthritis worldwide, one of the most prevalent sources of chronic musculoskeletal pain,⁴³ and a leading cause of disability.^{14,42} Pain is the defining symptom and primary complaint of OA,³⁷ and its consequences include fatigue, sleep disruption, reduced activity, and psychological stress.²⁷ Understanding the mechanisms of pain in OA is thus critical for the management of the disease.

Traditionally, OA was considered the hallmark of nociceptive pain, explained by mechanical and biochemical activation of

afferents innervating the affected joint.^{29,63} Recent studies show evidence for peripheral sensitization of nociceptors⁵⁹ and central sensitization, associated with nociceptive-mediated transmission strengthening and dysfunction of descending modulator pathways in OA.⁴¹ In addition, neuropathic-like symptoms,^{19,28} negative affect, anxiety, and catastrophizing have been related with pain severity,^{1,57} suggesting linkage between the brain's emotional circuitry and OA pain.

We^{6,7,38,46} and other researchers^{16,25,39} have provided evidence for brain anatomical and functional abnormalities in OA. Brain activity for ongoing OA pain⁴⁶ shows similar activity patterns as observed in chronic back pain (CBP).^{6,26} Disruption of information sharing,³⁸ and brain morphological distortions are reported both in OA and in CBP.⁷ Given that transition from subacute to CBP is predicted by brain anatomical and functional parameters^{8,62} and chronicification of back pain is accompanied by anatomical and functional reorganization,²⁶ a similar concept can be formulated for OA pain, namely, brain parameters in part predefine risk and consequently reorganize with OA pain. Here, we attempt to address this issue from the viewpoint of brain morphology. Hip OA (HOA) and knee OA (KOA) have distinct clinical characteristics, pain properties, and joint replacement surgery outcomes. For both conditions, pain is poorly related to joint structural damage.¹⁸ Our main hypothesis is that KOA and HOA exhibit brain gray matter (GM) distortions when contrasted with healthy controls, and GM properties should also be different between the 2 conditions.

GM indices indicate morphologic brain abnormalities in OA,^{2,25,34,39} but their clinical import is not yet understood. Although promising, these data are primarily derived from small samples at

Sponsorships or competing interests that may be relevant to content are disclosed at the end of this article.

^a Departamento de Biomedicina, Faculdade de Medicina, Instituto de Investigação e Inovação em Saúde-i3S, Universidade do Porto, Porto, Portugal, Departments of

^b Physical Medicine and Rehabilitation and, ^c Physiology, Feinberg School of Medicine, Northwestern University, Chicago, IL, United States, ^d Departments of Biomedical Engineering and Statistics, Northwestern University, Evanston, IL, United States, ^e Unilabs Boavista, Porto, Portugal, Departments of ^f Rheumatology and, ^g Anesthesia, Feinberg School of Medicine, Northwestern University, Chicago, IL, United States

*Corresponding author. Address: Feinberg School of Medicine, Northwestern University, Tarry Bldg. 7-705, Chicago, IL 60611, United States. Tel.: (312) 503-0404; fax (312)503-5101. E-mail address: a.apkarian@northwestern.edu (A.V. Apkarian).

Supplemental digital content is available for this article. Direct URL citations appear in the printed text and are provided in the HTML and PDF versions of this article on the journal's Web site (www.painjournalonline.com).

PAIN 161 (2020) 2167–2178

© 2020 International Association for the Study of Pain
<http://dx.doi.org/10.1097/j.pain.0000000000001904>

distinct stages of OA progression, and evidence is discrepant as GM changes exhibit little overlap between studies. Moreover, previous literature fails to find robust associations between clinical properties of OA and brain structural changes.^{2,39} Our second objective is to study the association between brain morphological distortions and OA clinical properties.

We study brain morphological distortions and their relationship with clinical outcomes in a large population of advanced KOA, and a smaller group of HOA, in contrast to healthy controls. We study GM properties at whole-brain voxel-wise scale and after subdividing gray matter to regions of interest (ROIs) and apply both univariable and multivariable machine-learning analysis to explore the multidimensional basis of these alterations. Finally, we perform a reverse inference mapping of obtained results to terms (using Neurosynth), providing a meta-analytic summary of results and linking brain anatomy to the psychological domain.

2. Patients and methods

2.1. Subjects

Advanced HOA and KOA patients with indication for total joint replacement were recruited in the Orthopedic Department of *Centro Hospitalar e Universitário de São João*, Porto, together with healthy controls from the same geographical area. Participant recruitment was finished at the time of this report. Sample size was determined by the number of patients waiting for surgery who met the eligibility criteria during a period of 20 months. Controls were recruited in the end of the patient recruitment phase and intended to be one-third of the patient number in the largest OA group.

Inclusion criteria for OA patients were: (1) age between 45 and 75 years; (2) diagnosis of HOA and KOA according to the clinical classification criteria of the American College of Rheumatology³; (3) surgical indication for total joint replacement. Exclusion criteria included: (1) secondary OA due to congenital and development diseases or inflammatory and autoimmune articular diseases; (2) bilateral OA with indication for contralateral arthroplasty in the following year or bilateral knee pain with less than or equal to 4 points difference on the numeric pain rating scale between knees; (3) other chronic pain conditions (eg, fibromyalgia; chronic pelvic pain), (4) chronic neurological or psychiatric disease; (5) previous history of stroke or traumatic brain injury.

Controls were subjects without chronic conditions, musculoskeletal disorders, and neurological disorders, from the same geographic area, age range, and social and educational background as the patients.

Clinical, demographic, and biopsychosocial measures were obtained 2 to 6 weeks before surgery and repeated at 3, 6, and 12 months after surgery, together with brain imaging collection (magnetic resonance imaging [MRI]). The study was approved by the local ethics committee, and all participants provided informed consent before partaking in the study. In this article, we are reporting baseline cross-sectional data from presurgical state. Longitudinal data results will follow in future work.

2.2. Clinical and behavioral measures

Demographic and clinical data were obtained at the initial interview and by clinical chart assessment. Bilateral radiographs of involved joints were performed as part of the standard hospital protocol and scored accordingly to the Kellgren–Lawrence classification³² by 2 trained radiologists. Physical performance was assessed with 2 distinct tasks—timed up and go test⁴⁷ and 6-minute walking test (6MWT).^{9,50}

All patients completed the following questionnaires: Knee and Hip Injury and Osteoarthritis Score (KOOS; HOOS)^{21,44,52}; Hospital Anxiety and Depression Scale (HADS)^{45,67}; Pain Catastrophizing Scale^{5,58}; and *Douleur Neuropathique en 4 questions*—Neuropathic pain scale (DN4).^{5,12} All questionnaires were used in their Portuguese validated versions.

2.3. Brain imaging

High-resolution, MPRAGE type T1-anatomical brain images were acquired with a 3.0 T Siemens Magnetom Spectra scanner (Siemens Medical, Erlangen, Germany). Acquisition parameters: isometric voxel size = 1 × 1 × 1 mm, TR = 2500 ms, TE = 3.31 ms, flip angle = 9°, in-plane matrix resolution = 256 × 256, number of slices, = 160; field of view = 256 mm. Total time of acquisition was 6 minutes.

2.4. Gray matter properties and statistical analyses

GM properties were extracted, and analyses were performed using tools from the Oxford Center for Functional Magnetic Resonance Imaging Software Library (FMRIB, Oxford OK; FSL version 5.0.10, <https://fsl.fmrib.ox.ac.uk/fsl>)³¹; Matlab (MATLAB 2018a; The MathWorks, Natick, 2018), and RStudio (RStudio Team (2016); RStudio: Integrated Development for R. RStudio, Inc, Boston, MA URL <http://www.rstudio.com>).

2.4.1. Total gray matter volume estimation

SIENAx (2.6) from FSL^{55,56} was used to calculate estimates of volumes of interest, after automated brain extraction and tissue segmentation. We compared total gray matter (GM) volume across groups using an analysis of covariance (ANCOVA), controlling for intracranial volume, age, and sex. Differential relationships between GM and age were assessed using linear regression, controlling for sex and total intracranial volume (TICV), in which a group interaction indicated a difference in slopes.

2.4.2. Voxel based morphometry

Regional GM density was analyzed with voxel-based morphometry (VBM) using tools from FSL. In brief, images were skull stripped using Brain Extraction Tool⁵⁵ and tissue-type segmented into GM, white matter, and cerebrospinal fluid using FMRIBs Automated Segmentation Tool.⁶⁶ A study-specific GM template was created using 72 gray-matter-segmented native images (24 subjects of each group; KOA and controls were randomly selected to minimize size of population bias). Steps towards the template creation included: affine registering the GM partial volume images (FLIRT)³⁰ and left-to-right x-axis flipping to produce a symmetrical image followed by nonlinear registration (FNIRT)⁴ to standard space. The native space GM volume images were then normalized into this template using a nonlinear registration (FNIRT) and corrected for the contraction/enlargement due to the nonlinear component of the transformation using the Jacobian. Finally, GM images were concatenated and smoothed with an isotropic Gaussian kernel (FWHM = 8 mm). Cerebellum was excluded from the analyses because the foci of this study were neocortical and subcortical structures.

A second group for parallel VBM analysis was created by midline flipping the scans of patients with left-sided OA (knee = 45; hip = 10), in accordance with previous OA and unilateral pain conditions studies.^{24,36} Brains were flipped along the x-axis

before nonlinear registration to the study template. All subsequent steps were identical.

Gray matter differences in OA groups and controls were assessed through a one-way between-subjects ANCOVA, using age, sex, and TICV, plus laterality of OA for the flipped data analysis as covariates of no interest. Permutation-based testing ($n = 5000$ permutations) was performed using FSL's randomize toolbox.⁶⁴ Threshold-free cluster enhanced uncorrected P -values were obtained,⁵⁴ and $\alpha = 0.001$ was used as threshold for statistical significance of group differences. A minimum cluster size of 66 voxels (number of voxels contained within the 8 mm smoothing kernel) was used as a secondary threshold. Post hoc analyses of VBM results using Tukey HSD tests for multiple comparisons of means were conducted for the identified clusters.

The association of significant clusters with clinical variables was examined using partial correlations, with age, sex, and TICV as covariates.

In addition to assessing simple group differences, we sought to understand their relationship with clinical variables. Thus, the association of significant clusters with clinical variables was examined using partial Pearson correlations, which controlled for age, sex, and TICV.

2.4.3. Regional Brodmann area parcellation-based analysis of gray matter GM morphometry volume

Next, we calculated GM volume for 90 cortical and subcortical ROIs approximating Brodmann areas, defined anatomically by the Automated Anatomical Labeling atlas (Neurofunctional Imaging Group [GIN-IMN] <http://www.gin.cnrs.fr/en/tools/aal/>).⁶¹ Cerebellum and vermis areas were excluded from the analysis. A list of regions, labeling, and respective coordinates can be found in Table S1 (available online as supplemental digital content at <http://links.lww.com/PAIN/B8>).

The volume of each ROI was calculated as the mean GM volume of all voxels within the ROI for each subject. Volumes were calculated both for native brains and x-axis-flipped brains depending on laterality of OA. Univariable analyses were conducted using one-way ANCOVA test for each region contrasting the 3 groups: KOA, HOA, and controls, while controlling for age, sex, and TICV. For the flipped brain analysis, laterality was also added as a covariate. Again, an $\alpha = 0.001$ was used a threshold for statistical significance of group differences. Multiple comparison correction was performed using a false discovery rate-adjusted P -value of 0.05.

Next, a multidimensional approach using a L1-regularized logistic regression (ie, least absolute shrinkage and selection operator [LASSO])⁶⁰ was performed. First, we divided our KOA sample into 2 distinct sets, training ($n = 46$) and test ($n = 45$). This was performed using the Kennard–Stone algorithm,³³ which allowed us to select samples with a uniform distribution over a multivariate predictor space (here: age, sex, pain levels, and behavioral variables). Second, using the KOA training set, we performed a logistic model with a LASSO penalty to predict group membership (ie, knee vs controls), based on the GM volumes of all 90 ROIs. In addition, we added age, sex, and TICV to the full model. Ten-fold cross-validation was used to choose the hyperparameter, λ , which minimized binomial deviance over a default grid size of 100.²⁰ Finally, models were evaluated in the KOA test group and HOA group by constructing receiver operating characteristic curves and computing areas under the curve (AUC).

Later, Neurosynth term-based reverse inference was used to decode the identified AAL regions for the flipped brain model. This meta-analytical tool contains a database with activation

coordinates for a total of 14,371 functional MRI studies (September 2019), paired with their associated cognitive and anatomical terms (<http://neurosynth.org/decode/>).^{22,48,65} The decoder takes in the voxel-wise representation of the ROI, cross-references it with the full database, and returns a list of terms and correlation values, which indicates the strength of terms associated with delineated brain regions, in contrast to the rest of the brain. Here, we retrieved the top 40 nonanatomical terms (of about 1700 terms generated) showing the greatest correlation with the model's ROIs. Next, to further elucidate the contribution of each region in the model, the correlation for each ROI was weighted by its LASSO-derived coefficient and ranked. Terms were visualized using a word-cloud (MATLAB 2018a and Text Analytical Toolbox, The MathWorks, Natick, 2018).

Finally, we aimed to test whether the OA classification models were associated with OA clinical variables.

For this, using the KOA testing group, we linearly modeled each clinical variable of interest with the variables retrieved from the LASSO. For statistically significant relationships ($P < 0.05$), the relative importance of each independent variable was calculated using the sequential sums of squares over all orderings of regressors,³⁵ and confidence intervals computed over 1000 bootstraps for each regressor.²³ Finally, statistically significant regression models were tested in the KOA validation group and HOA group by calculating Pearson correlation coefficient between predicted and real values.

3. Results

3.1. Demographic and clinical characteristics

A total of 91 KOA patients, 24 HOA patients, and 36 healthy controls were included in the study. Patient and control groups were similar concerning education, habitation profile, marital status, and smoking habits. Age and sex were statistically significantly different among the 3 groups: age was higher in the KOA group and HOA had a lower representation of females.

Pain intensity as well as affective measures and performance-based tasks did not statistically significantly differ among OA groups. The KOA group, however, presented a longer pain duration and a higher probability of neuropathic pain than the HOA group, which in contrast exhibited higher radiographic structural damage (Table 1).

3.2. Total gray matter characterization

Total neocortical gray matter volumes (TGM) were compared between the 3 groups (OA and controls), while controlling for TICV, age, and sex. TGM was not statistically significantly different between the 3 groups ($F(2,145) = 0.07$, $P = 0.79$). Women showed greater TGM than men (controlling for group, TICV, and age) (Fig. 1A). The effect of age on TGM was calculated for each group separately (after correcting for sex). TGM decreased with age (Fig. 1B) and the interaction between age and group was not statistically significant ($F(2,145) = 2.62$, $P = 0.078$), showing approximately similar trends for the 3 groups.

3.3. Hip osteoarthritis patients exhibit lower GM volume in anterior cingulate/paracingulate cortex

To identify regional differences in GM volume between OA groups and controls, we performed a whole-brain, voxel-wise, one-way ANCOVA for VBM outcomes (Fig. 1C). Statistically significant differences in GM volume in the right and left anterior cingulate

Table 1**Demographic and clinical characteristics of osteoarthritis patients and controls.**

	Controls	Knee OA	Hip OA	P
Subjects, n, %	36	23	91	16
Age (y), mean, SD	59.2	8	65.5	6.5
Female, n, %	20	55.5	72	79.1
BMI (kg/m ²), mean, SD	27.8	4.6	30.4	4.9
Education, n, %				0.12
Primary education	21	58.3	71	78
Secondary education	8	22.2	15	16.5
Post-secondary education	7	19.5	5	4.5
Post-secondary education				12.5
Smoking, n, %	8	22.2	8	8.8
Habitation, n, %				
Alone	6	16.7	17	18.7
Cohabitation	30	83.3	74	81.3
Marital status, n, %			6	
Married	27	66.7	65	71.4
Never married	3	8.3	5	5.5
Divorced	2	5.6	7	7.7
Widowed	4	11.1	14	15.4
Pain duration (y), mean, SD	—	—	7.7	6
Pain intensity (NRS), mean, SD	—	—	6.6	1.7
KOOS/HOOS, mean, SD	—	—	61.2	20
Symptom	—	—	63.7	15.6
Pain ADL SR	—	—	62.6	16.4
QoL	—	—	91.9	13.9
	—	—	79.5	15.3
			71.1	20.3
HADS, mean, SD				0.354
Anxiety	—	—	8.8	5
Depression	—	—	7.1	4.1
PCS, mean, SD			8.3	4.8
Rumination magnification	—	—	5	3.7
Helplessness	—	—	10	7.5
DN4, mean, SD	—	—	2.8	2.2
Physical performance tasks, mean, SD				
TUG, seg	—	—	13.6	4.2
6MWT, meters	—	—	14.4	4.7
Radiographic KL, n, %				<0.001†
Grade 1	—	—	2	1.8
Grade 2	—	—	21	23.1
Grade 3	—	—	43	39.1
Grade 4	—	—	25	22.8
			18	75

To identify demographic difference between groups, ANOVA and t-tests were performed for continuous data, controls and OA groups, and between OA groups, respectively. χ^2 tests were performed for categorical data.* $P < 0.05$.† $P < 0.001$.

6MWT, 6-Minute Walking Test; ADL, activities of daily living; ANOVA, analysis of variance; BMI, body mass index; DN4, Douleur Neuropathique en 4 questions; HADS, Hospital Anxiety and Depression Scale; HOOS, Hip Injury and Osteoarthritis Outcome Score; KOOS, Knee Injury and Osteoarthritis Outcome Score; KL, Kellgren–Lawrence scale; NRS, numeric pain rating; PCS, Pain Catastrophizing Scale; SR, sports and recreation; TUG, stand up and go test; QoL, quality of life.

cortex/paracingulate gyri were identified, differentiating the 3 groups (**Table 2**). Post hoc analyses (Tukey HSD test) revealed statistically significantly reduced regional volume only for HOA when compared with KOA and controls ($P < 0.001$). Knee osteoarthritis and controls did not show a statistically significant difference within this cluster ($P = 0.34$).

3.4. Hip osteoarthritis and knee osteoarthritis patients exhibit lower GM volume in primary motor cortex contralateral to osteoarthritis pain

Next, we sought to isolate the effects of OA pain on regional GM volumes. To this end, we first realigned the OA brains relative to

the body part with OA pain. That is, brains were flipped across the midsagittal plane for left-side OA patient (x-axis flipping), such that the left hemisphere would correspond to the body side contralateral to OA pain for all patients. We then performed whole-brain, voxel-wise analyses using one-way ANCOVAs across the 3 groups for VBM outcomes. Using the same criteria for statistical significance as above (ie, $\alpha = 0.001$), we identified 5 statistically significant clusters (**Fig. 2A** and **Table 2**). Post hoc analysis of these clusters revealed: (1) relative to healthy controls, both OA groups exhibited lower volumes in left primary motor cortex (precentral cortex), as well as in the left temporal pole; and (2) relative to healthy controls, KOA, but not HOA, had lower GM volume in the precuneus cortex and increased GM volume in the

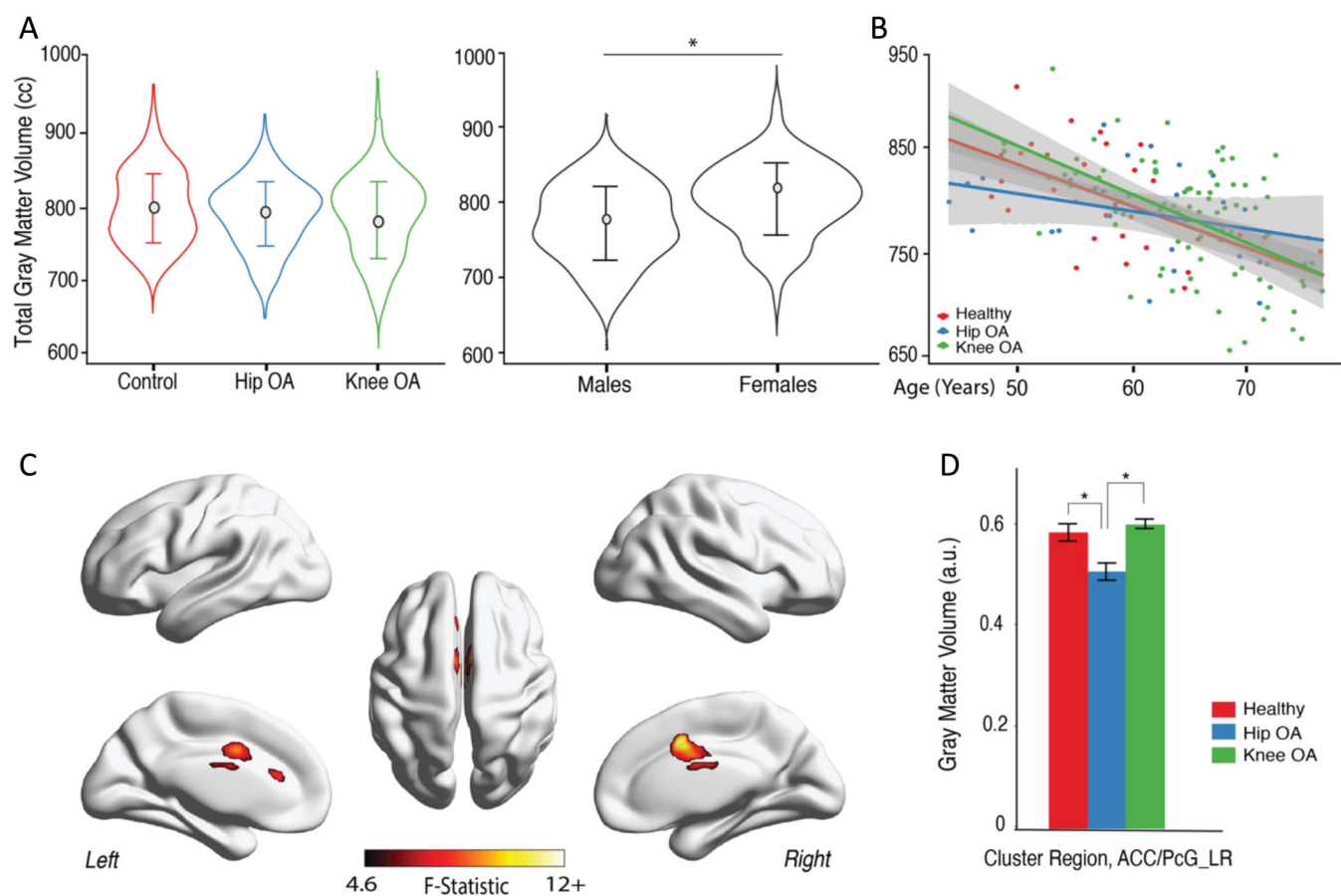


Figure 1. Whole-brain cortical gray matter changes reflect lower volumes in anterior cingulate, paracingulate gyri in HOA. (A) Average total neocortical gray matter (TGM) matter volume was not different between healthy controls, HOA, and KOA patients (age, sex, and intracranial volume were used as confound variables ($F(2,145) = 0.07, P = 0.79$)). TGM differed by sex across groups, when controlling for total IC volume and age ($F(1,145) = 15.7, P < 0.001$), with females showing higher volumes. (B) Scatterplot represents total neocortical GM in relation to age for each subject, color-coded by group; slopes were computed for each group, showing decrease of TGM with age, for all groups ($P < 0.05$; R2: controls = 0.52; KOA = 0.37; HOA = 0.17). (C) Gray matter morphological changes assessed by voxel-based morphometry (VBM). The 3 groups were contrasted together, using a 1-way between-subjects ANCOVA, with age, sex, and total ICV as covariates of no interest. Shown is the F-test statistical map, clustering determined using uncorrected P -value binarized at value of 0.001 and cluster size >66 voxels. Only cingulate/paracingulate gyri showed regional GM volume difference between the groups. (D) Post hoc results for GM volume comparisons in the identified region—anterior cingulate/paracingulate gyri (ACC/PcG_LR). Bars represent the mean gray matter volume and error bars represent the standard error. Tukey HSD test showed regional GM volume was lower in HOA from KOA and healthy subjects at $P < 0.001$. Knee osteoarthritis and controls did not show a statistically significant difference ($P = 0.34$). * $P < 0.001$. ANCOVA, analysis of covariance; HOA, hip osteoarthritis; KOA, knee osteoarthritis.

medial frontal gyrus. In addition, we identified lower GM volume in the anterior cingulate cortex (ACC_LR) for the HOA group relative to KOA and controls. This cluster considerably overlapped (Sørensen–Dice coefficient = 0.71) with the ACC cluster we obtained in the nonflipped analysis. The unthresholded statistical maps for native space and flipped analysis can be accessed in NeuroVault.org (<https://identifiers.org/neurovault.collection:6002>).

Overall, by aligning the brain in relation to body side with OA pain, we observe more statistically significant clusters and stronger effects of GM volume differences between the groups. Importantly, we are able to identify the primary motor cortex region contralateral to the OA pain with lower GM volume in both knee and HOA patients.

3.5. Lack of relationship between clinical variables for clusters identified by voxel-based morphometry

To elucidate the clinical relevance of the GM volume differences among HOA, KOA, and healthy controls (6 clusters, before and after brain flipping), we correlated clinical characteristics of OA

with GM volumes. The relationship between cluster GM volumes and clinical variables was calculated using partial correlations, controlling for age, sex, and TICV. We did not find any statistically significant relationships ($|r| \leq 0.28$; (Table S2, available online as supplemental digital content at <http://links.lww.com/PAIN/B8>).

3.6. Univariable and multivariable GM volume relationships associated with osteoarthritis, after parcelling the brain into Brodmann areas

The above analyses were done at the voxel level. To reduce dimensionality, we studied GM properties across the groups and as a function of clinical characteristics after parcelling the brain into ROIs approximating Brodmann areas (AAL atlas). GM volume differences were studied at this larger scale by subdividing the brain into 90 predefined regions (approximating 45 left and 45 right brain Brodmann areas) and calculating the mean GM volume for each ROI. Reduced dimensionality enabled studying OA-related brain volume differences with a multivariable approach, which considers the inter-relationships between regional GM volumes.

Table 2

Clusters for GM volume differences in HOA, KOA, and healthy controls for whole brain analysis with and without brain flipping based on OA body side dominance (x-axis).

Peak MNI coordinate region (Harvard-Oxford Cortical Structural atlas)	Peak (max) F value	No. of voxels	Peak MNI coordinate
Nonflipped brain (Fig. 1C)			
Paracingulate gyrus (20%); cingulate gyrus, anterior division (14%); juxtapositional lobule cortex (7%)	12.4	888	(12,8,8)
Cingulate gyrus, anterior division (93%)	8.58	51	(−2,32,16)
Flipped brain (Fig. 2A)			
Cingulate gyrus, anterior division (9%), posterior division (4%)	18.8	1224	(8,−8,32)
Precentral gyrus (54%)	7.55	136	(−28,−18,70)
Temporal pole (34%)	9.06	122	(34,8,−34)
Precuneous cortex (49%), intracalcarine cortex (72%)	13.2	84	(12,−58,10)
Middle frontal gyrus (42%), superior frontal gyrus (2%)	10.3	76	(30,24,50)
Middle frontal gyrus (23%), superior frontal gyrus (2%)	8.45	30	(−38,2,64)
Frontal orbital cortex (88%)	10.5	27	(−22,26,−20)
Heschl gyrus (22%)	10.9	24	(−42,−28,8)
Precentral gyrus (64%), middle frontal gyrus (2%)	6.72	14	(−52,−4,50)

All identified clusters from VBM GLM analysis, TFCE uncorrected $P < 0.001$. Cluster peak coordinates (x,y,z) are displayed according to MNI atlas, labels according to the Oxford-Harvard Structural Cortical Atlas (<http://fsl.mrc-cbu.cam.ac.uk/fsl/fslwiki/Atlases>). We accepted clusters greater than 66 voxels in size for post hoc analysis, given the Gaussian Kernel (FWHM = 8 mm) used for smoothing.

HOA, hip osteoarthritis; KOA, knee osteoarthritis; OA, osteoarthritis; VBM, voxel-based morphometry.

First, differences in GM volume across the 3 groups were examined for each ROI in the native and appropriately flipped brains (rendering OA pain to be left body side lateralized) using a one-way ANCOVA (**Figs. 3A and B**). Multiple regions that attained statistical significance were identified ($P < 0.001$): left putamen in the native brain analysis; bilateral pallidum, precentral left cortex, and 2 right frontal regions (rectus and lingual gyrus) for the flipped brain analysis. After FDR correction for multiple comparisons, only left precentral cortex yielded statistical significance ($F = 5.9$, corrected $P < 0.05$). Post hoc analysis for this ROI showed decreased volume for both OA groups when

compared with controls (Tukey HSD tests, $P < 0.01$), but not between OA groups ($P = 0.73$), showing a pattern concordant with the results obtained in the voxel-wise analysis.

We next sought to study GM volumetric differences in a multivariable space using logistic regression to classify OA patients and controls based on 90 ROIs. To enforce sparsity and reduce overfitting, we used L1 regularization (LASSO) to drive coefficients towards zero. We took advantage of the large number of KOA patients and subdivided this group into training and test groups to ensure generalizability and unbiasedness. Results obtained in the training group were tested on the hold-out

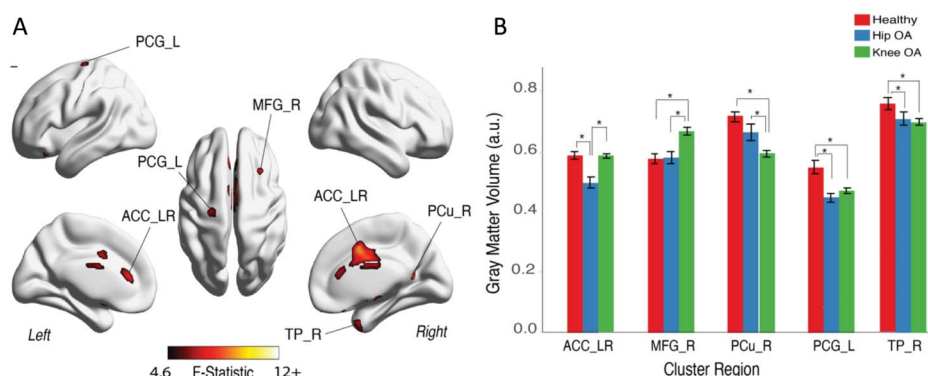


Figure 2. Primary motor cortex, contralateral to OA pain, showed lower volume in both HOA and KOA patients. (A) Gray matter morphological changes assessed by voxel-based morphometry (VBM) after aligning the brain in relation to OA pain (brain x-axis left-to-right flipping for left-sided KOA and HOA, which renders the left hemisphere to be contralateral to OA in all patients). The 3 groups were contrasted together, using a 1-way between-subjects ANCOVA, controlling for age, sex, total ICV, and brain flipping. Shown is the F-test statistic map clustering determined using a TFCE uncorrected P -value binarized mask at a value of 0.001 and cluster size >66 voxels. Multiple brain regions showed changes in regional volume (B). Post hoc results for GM volume differences for significant clusters, adjusted for age, sex, and TICV (Tukey HSD tests at $P < 0.001$); bars represent the mean gray matter volume and error bars represent the standard error. Left primary motor cortex (precentral gyrus; PCG_L) and right temporal pole (TP_R) presented lower GM volume in both OA groups. Bilateral anterior cingulate cortex (ACC_LR) showed lower GM volume only in HOA, when contrasted with the other 2 groups. In the KOA group, GM volume was greater for middle frontal gyrus cluster on the right (MFG_R) and lower for right precuneous cortex (PCu_R). Further information on thresholded clusters can be found in Table 2. * $P < 0.001$. HOA, hip osteoarthritis; KOA, knee osteoarthritis; OA, osteoarthritis; TICV, total intracranial volume.

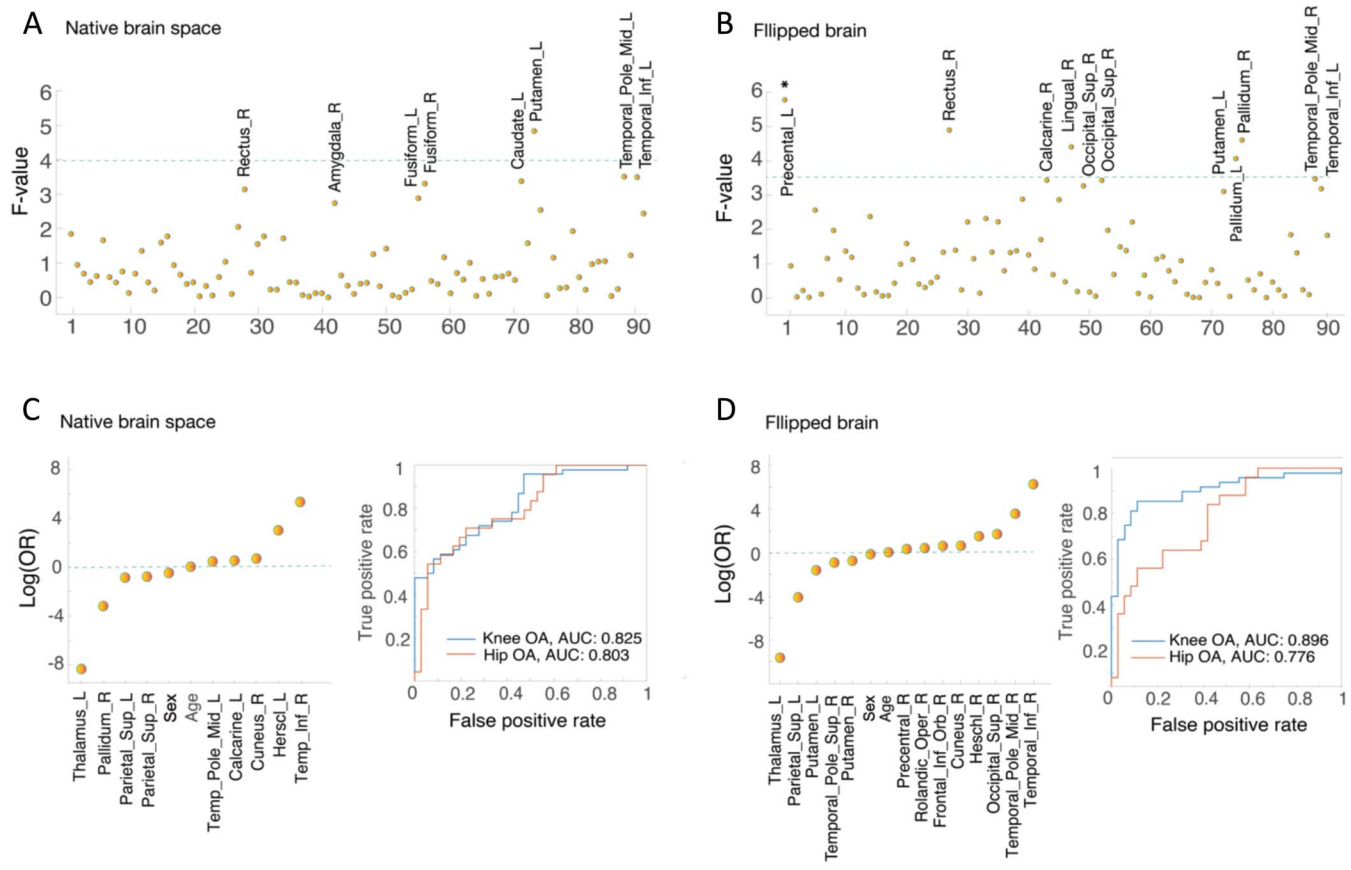


Figure 3. Univariable and multivariable analysis of regional GM differences between groups. Cortex was subdivided into 90 ROIs approximating Brodmann areas, using the AAL atlas; A and B plots show the F-value for each ROI across group comparison in native space, without brain flipping (A) and after flipping the brains (B) based on OA body side dominance (x-axis). Age, sex, TICV, and OA side in lateralized analysis were entered as covariates of no interest. Green line indicates uncorrected significance threshold at $P < 0.01$ ($F(3,148) > 4$ and $F(4,127) > 3.5$ for A and B); brain regions above and close to uncorrected threshold are labeled and include subcortical regions, temporal, and frontal regions. Primary motor cortex was identified solely in the flipped brain analysis (B) and was the only region surviving FDR correction for multiple comparisons (* $P < 0.05$). (C and D) The coefficient estimates (log(Odds)) in KOA training group after LASSO regularization with lambda selection through 10-fold cross-validation for native (C) and in flipped volumes (D). Receiver operating characteristic for classification by logistic regression for the test KOA group and HOA group are also reported (blue = KOA; red = HOA). Areas under the curve showed values between 0.77 and 0.90, suggesting that generated models were not overfit and selected parameters are relevant predictors of OA-related brain morphological properties. HOA, hip OA; KOA, knee OA; OA, osteoarthritis; LASSO, least absolute shrinkage and selection operator; ROI, region of interest; TICV, total intracranial volume.

test group. **Figures 3C and D** show multivariable model results for the training KOA sample in native space (**Fig. 3C** left panel) and for flipped brain analyses (**Fig. 3D** left panel). Age and sex, although having small influences (0.24–0.06 log(OR)) were captured in both models. In addition, the combination of lower GM volumes of the left thalamus and parietal superior left cortex and higher GM volumes of temporal inferior gyrus together were strong predictors for KOA classification in both models. The flipped brain model captured additional regions not observed in the native analysis, including lower GM volumes in bilateral putamen, and higher GM volumes in right precentral gyrus and in frontal inferior orbital gyrus.

We tested the performance of the classification models in the KOA hold-out sample to test validity of obtained results, and in HOA sample to test for generalization from KOA to HOA. For the hold-out KOA group, an AUC of 0.82 (nonflipped analysis) and 0.89 (flipped brain analysis) was attained. When evaluated in the HOA group, logistic regression presented an AUC of 0.8 and 0.77 for nonflipped and flipped analyses, respectively. Receiver operating characteristic curves are displayed in **Figure 3C** (right panel) and **Figure 3D** (right panel). Probability plots for each model are presented in Figure S1 (available online as supplemental digital content at <http://links.lww.com/PAIN/B8>).

Finally, we tested the model's performance for classifying among OA groups. The obtained AUC's were 0.65 and 0.76 for the nonflipped and flipped models, respectively (probability plots, Figure S2, available online as supplemental digital content at <http://links.lww.com/PAIN/B8>). Multivariable models seem both valid and generalizable from KOA to HOA, with the flipped model showing higher specificity for KOA.

3.7. Neuropathic pain associated with multivariable model for knee osteoarthritis

Given that the flipped brain multivariable model could better distinguish between OA and healthy controls, also showing higher specificity for knee OA, we further examined this model (**Fig. 4A**). First, we used Neurosynth database meta-analytical decoding to identify psychological/task terms associated with brain activity in these regions. We decoded the regions as absolute values, reflecting only location (**Fig. 4B**), and also using weighted values to account relative contribution of different regions in the model (**Fig. 4C**). The top 5 terms associated with the model for location only were: dementia, personality, gestures, social interaction, and interpersonal relations. When incorporating the model coefficient of each area, the main terms identified were pain, anticipatory, finger tapping, index finger, and integrate.

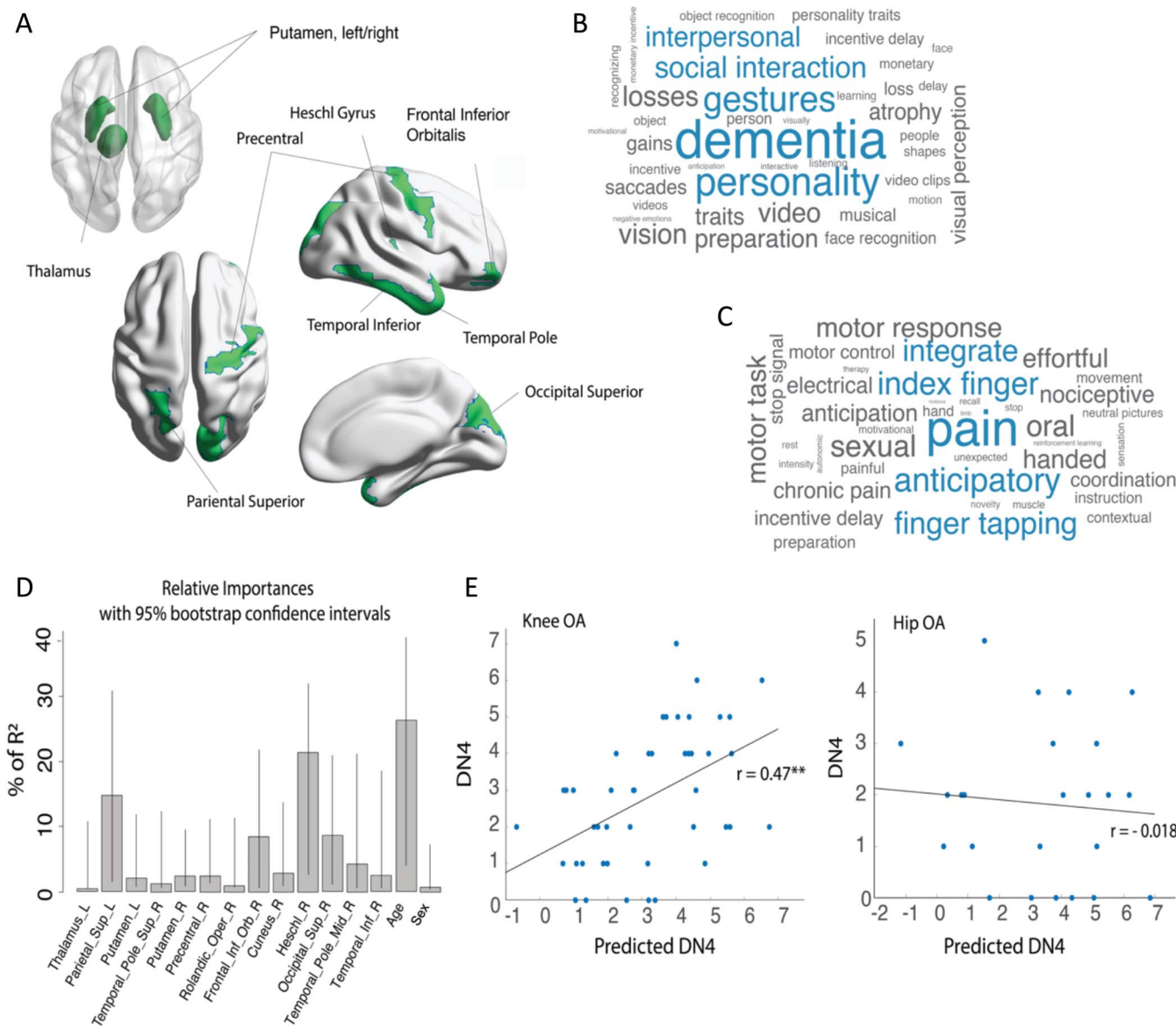


Figure 4. Neuropathic pain profile was associated with KOA multivariable brain volume changes. (A) Graphic representation of the AAL ROIs identified in the multivariable analysis (flipped brain). (B and C) plots show the top 40 (of about 1700) correlated psychological/task terms using Neurosynth reverse inference decoder for the brain regions (B) and weighted regions, given the model estimate coefficients (C). The size of a term in each word cloud is proportional to the correlation strength of term/region. Blue color represents top 5 correlations. (D–E) A multiple regression model using the logistic regression/LASSO results for flipped brain KOA classification predicted neuropathic pain score (DN4) in a subsample of KOA patients (training sample, $n = 45$). This result was validated on a KOA hold-out sample (test sample, $n = 46$), but not in the HOA group. (C) The relative importance of all predictive variables where % of R^2 is normalized to sum 100%. Bars correspond to 1000 bootstrap confidence intervals at 95%. (E) The validation of the obtained regression model in KOA testing sample and HOA groups. Predicted neuropathic pain scale (DN4) strongly and significantly correlated with the actual score in the KOA test group, but not in the HOA. DN4 (Douleur Neuropathique en 4 questions); ** $P < 0.001$. HOA, hip osteoarthritis; KOA, knee osteoarthritis; LASSO, least absolute shrinkage and selection operator; ROI, region of interest.

In an unbiased approach, we tested the model's association with clinical aspects of pain and mobility in OA. Using the KOA training sample ($n = 45$), and the predictors obtained from the LASSO, multiple regression models were built for each clinical variable of interest (ie, pain duration; pain intensity; HADS anxiety; HADS depression; Pain Catastrophizing Scale; 6MWT; timed up and go; DN4 and KOOS subscales). Only one model yielded statistical significance: neuropathic pain scale, DN4 ($F(1,45) = 2.29$; $Adj R^2 = 0.29$; $P = 0.03$). Details for all generated models can be found in Table S3 (available online as supplemental digital content at <http://links.lww.com/PAIN/B8>). Finally, because several models were generated and thus spuriousness of the DN4 model is highly feasible, we sought to better characterize and

unbiasedly validate the DN4 model. To do so, we first calculated the relative importance for each predictor variable and computed its respective 95% confidence interval using 1000 bootstrap replicates (Fig. 4D). Age, parietal superior cortex, Heschl/S2 gyrus, and frontal inferior orbitalis cortex presented the highest percentage of explained variance, with smaller contributions from other brain regions. We then validated the model in the KOA hold-out sample ($n = 45$), where the correlation between DN4 and predicted DN4 was statistically significant and strong ($r = 0.47$, $P < 0.001$). The model failed to replicate in the HOA group ($r = -0.018$, $P = 0.93$; Fig. 4E). Therefore, the obtained multivariable model reflects neuropathic pain characteristics, and the model is valid for neuropathic pain in KOA but does not generalize to HOA.

4. Discussion

Our univariate analyses highlight primarily lower GM volume in HOA in the anterior cingulate, and lower GM volume in the precentral cortex in both KOA and HOA contralateral to OA pain. In addition, the multivariable analysis reveals GM distortions captured as a multidomain system that integrates cortical and subcortical structures, shared between KOA and HOA. Reverse inference of this multidomain distortion, from functional brain space to psychological and task-related terms, identified 2 sets of concepts: (1) for unweighted location analysis associated terms included dementia, personality, gestures, social interaction, and interpersonal relations; (2) when the same analysis was performed taking into consideration the weights of contributing regions, the top associated concepts were: pain, anticipatory, finger tapping, index finger, and integrate. We found that the multivariable set of regions was associated with patient-reported neuropathic pain in KOA, but not in HOA patients. Importantly, the latter group has shorter pain duration and lower neuropathic pain scores. Our univariable analysis demonstrates more widespread and stronger GM distortions when taking into account the laterality of OA; however, no statistically significant relationships were found between univariable (VBM) results and clinical variables, similar to previous reports in the field.^{2,39}

Brain structural changes using GM indices in chronic pain have been reported by multiple groups, primarily using VBM. Disparate regions, both directions of GM change, and even null findings are reported.¹³ Our study was designed with the purpose of characterizing brain structural properties in the largest OA population reported to date. Our results are, in part, consistent with earlier reports: decreased GM in ACC seen in HOA has also been described in the past⁵¹; decreased precentral GM seen here in KOA and HOA is consistent with a report of functional remodeling of the motor cortex in KOA patients.⁵³ Importantly, we did not observe significant GM changes (univariable analysis) in brain areas previously reported for OA VBM studies, including both subcortical (thalamus,²⁵ amygdala and nuclei accumbens,³⁴ and caudate nuclei³⁹) and cortical areas (insular cortex and dorsolateral prefrontal cortex⁵¹). Incongruent findings across studies may relate to the heterogeneity of OA pain at distinct stages of the disease, but also to the potential inherent limitations of VBM; eg, the sensitivity of VBM to imaging parameters and scanner differences, in addition to analytical details, such as spatially normalizing atypical brains and limitations of univariate techniques.^{7,40}

Our multivariable analysis indicates the existence of a common set of brain distortions between KOA and HOA that differentiate these patients from healthy controls: 9 to 13 brain areas, composed of both cortical and subcortical regions. There is accumulating evidence that chronic pain leads to whole-brain global reorganization.¹³ Tested specifically in OA patients, pain was associated with whole-brain degree rank order disruption,³⁸ and changes in large-scale brain network temporal dynamics.¹⁶ Bridging this concept to morphologic brain reorganization in OA, we examined the GM volumetric distortions in a multidimensional space, accounting for the interrelationship between regions. Classification models were generated in a KOA sample, both in native and flipped brain space, and tested in hold-out KOA and HOA groups. Interestingly, the native space model yielded similar accuracy for knee and hip patients. Accuracy improved for the KOA group in the flipped brain space.

To better characterize this model, we identified the terms in the brain imaging literature associated with these regions using Neurosynth Image Decoder and selected the top 40 (of about

1300 terms) nonanatomical terms. The method uses meta-analysis (exploring around 14,000 brain imaging studies) to identify psychological and task-related terms associated with the collection of brain regions included in the multivariable model. The reverse association for the unweighted multivariable model identifies cognitive, interpersonal, and social interaction concepts, not obviously related to OA. Remarkably, when the weighted multivariable model was examined, the top term was pain (chance probability of this observation is near 1 in 1300 = 0.0008); additional pain-related terms, including chronic pain as well as motor-related terms, were also captured. This result is noteworthy because Neurosynth explores brain activity in a heterogeneous population and yet identifies pain and motor properties in the weighted multivariable model.

When studying the relationship between clinical measures and LASSO-derived multivariable models, we show that neuropathic pain probability, measured with the DN4 scale, is associated with the set of identified variables in the KOA group. Using an unbiased approach, we demonstrated that this result validates in the KOA sample but fails to generalize for HOA patients. This finding deserves a thorough examination: (1) KOA patients show a higher probability of neuropathic pain than HOA, fact that has been previously described¹¹; (2) interestingly, in our sample, KOA patients also showed a longer pain duration, but less severe radiographic damage.

These results are concordant with Dabare et al.,¹⁷ who showed that HOA symptomatology clinically presents later with more advanced disease than KOA, and patients are likely to undergo arthroplasty earlier from the time of presentation. Our findings suggest that, together with longer pain duration, there is the emergence of a neuropathic pain profile that can be clinically identified and linked to brain GM morphological properties. Our present result cannot unequivocally establish whether the multivariable GM distortion is a prognostic or diagnostic of neuropathic pain. However, the temporal dissociation between knee and hip pain and radiographic damage, together with a shared GM multivariable model, suggests that the model is more likely to be prognostic risk factor for developing signs of neuropathic pain in OA.

In a recent report based on the same KOA and HOA patient cohort, we examined the relationship between OA pain and clinical parameters.¹⁰ Although multiple models could be derived for different measures of OA pain, these were not consistent and thus were deemed unstable and uninformative. Here, we queried the univariate and multivariable GM distortions associated with OA regarding their relationship to clinical characteristics. Univariate brain distortions were more prominent in the hemisphere contralateral to OA pain, and the neuropathic pain scale was related to the multivariable model, yet the majority of clinical parameters associated with OA were unrelated to GM distortions. This raises the question whether observed GM distortions can be seen as prognostic or diagnostic. Within the conceptual construct of the four-stage model for transition to chronic pain,⁴⁹ formulated based on a longitudinal study of back pain patients,⁸ we have proposed a set of criteria that would differentiate between prognostic and diagnostic biomarkers for chronic pain: prognostic biomarkers should be preexisting factors that influence transition to chronic pain but are not modulated by pain. Conversely, diagnostic biomarkers are emergent in time with the transition to chronic pain and should reflect pain and related clinical characteristics. If we presume that the transition to chronic pain for OA, relating to its persistence after joint replacement surgery, follows the same general model as in back pain, then a lack of relationship

between clinical parameters and GM abnormalities suggests these are more likely to be prognostic in nature. This notion should be especially true for brain regions or multivariable models that show distortions shared between KOA and HOA as the impact of OA pain in HOA is distinct from that for KOA,¹⁰ which in turn should differentially distort GM in areas reflecting diagnostic consequences.

This study does not come without limitations. Results from the VBM analysis should be cautiously interpreted because identified clusters result from uncorrected whole-brain analysis; however, our report is in line with previous publications on brain morphometry in chronic pain, reporting group comparisons at uncorrected $P < 0.001$.² We limit reporting only large cluster GM abnormalities (>66 voxels) to minimize false-positive findings. Another important limitation that has to be highlighted is the imbalance in the number of subjects between OA groups and controls. Although such an imbalance limits our statistical power,¹⁵ our knee group was sufficient to construct the multivariable models using half of the knee patients. However, this is in contrast to the control group, which was not large enough to split, and thus, it was used in both the training and test set. Another shortcoming of this study is the fact that controls are not perfectly matched regarding age and sex with our KOA group; however, we account for the effect of these variables in all stages of our analysis. Finally, socioeconomic and cultural differences regarding attitudes of coping and/or suffering with OA pain may also underlie differences in VBM results when contrasting our findings with other studies.

In conclusion, our results show decreased GM in HOA in the ACC and decreased GM in precentral cortex in both KOA and HOA; however, these GM differences are not strongly correlated with clinical variables in OA. Moreover, we derived a multivariable model based on GM distortion that differentiated OA patients from healthy subjects. Importantly, this model was associated with the neuropathic scale in KOA, and in reverse inference, it was linked with pain and motor control in the brain imaging literature. We reason that observed GM distortions may reflect a priori risks for chronicity of OA pain rather than being consequential to the development of the disease.

Conflict of interest statement

The authors have no conflicts of interest to declare.

Acknowledgements

The authors thank to Dr Paulo Oliveira, for the clinical support and supervision of patients enrolled in the study, and all the members of the Orthopedic Department of Centro Hospitalar Universitário de São João, Porto, for their support with data collection. The authors thank Unilabs Boavista and Dr Nuno Martins for all the support in imaging data acquisition. The authors are thankful to all Apkarian laboratory and Galhardo laboratory members who contributed to this study with their time and resources.

J. Barroso was funded through CCDRN [Norte-08-5369-FSE-000026], OARSI Collaborative Scholarship 2018 and Luso-American Development Foundation R&D scholarship grant. Neuroimage data acquisition was provided by Unilabs Boavista and the Grünenthal Young Pain Researcher 2017 Grant, Portugal. This material is based upon work supported by the National Science Foundation Graduate Research Fellowship under Grant No. DGE-1324585.

Appendix A. Supplemental digital content

Supplemental digital content associated with this article can be found online at <http://links.lww.com/PAIN/B8>.

Supplemental video content

A video abstract associated with this article can be found at <http://links.lww.com/PAIN/B9>.

Article history:

Received 24 January 2020

Received in revised form 16 March 2020

Accepted 1 April 2020

Available online 4 May 2020

References

- Akin-Akinyosoye K, Frowd N, Marshall L, Stocks J, Fernandes GS, Valdes A, McWilliams DF, Zhang W, Doherty M, Ferguson E, Walsh DA. Traits associated with central pain augmentation in the Knee Pain in the Community (KPIc) cohort. *PAIN* 2018;159:1035–44.
- Alshuft HM, Condon LA, Dineen RA, Auer DP. Cerebral cortical thickness in chronic pain due to knee osteoarthritis: the effect of pain duration and pain sensitization. *PLoS One* 2016;11:e0161687.
- Altman R, Asch E, Bloch D, Bole G, Borenstein D, Brandt K, Christy W, Cooke TD, Greenwald R, Hochberg M, Howell D, Kaplan D, Koopman W, Longley S, Mankin H, McShane DJ, Medsger T Jr, Meenan R, Mikkelsen M, Hochberg W, Mqscowitz, Murphy W, Rothschild B, Segal M, Sokoloff L, Wolfe F. Development of criteria for the classification and reporting of osteoarthritis. Classification of osteoarthritis of the knee. Diagnostic and Therapeutic Criteria Committee of the American Rheumatism Association. *Arthritis Rheum* 1986;29:1039–49.
- Andersson JLR, Jenkinson M, Smith S. Non-linear registration, aka spatial 524 normalisation. *FMRIB Tech Rep* 2010:TR07JA2. Available at: <https://www.fmrib.ox.ac.uk/datasets/techrep/tr07ja2/tr07ja2.pdf>
- Azevedo LCP. Tradução, adaptação cultural e estudo multicêntrico de validação de instrumentos para rastreio e avaliação do impacto da dor crônica (Translation, cultural adaptation and multicentric validation study of chronic pain screening and impact assessment instruments). *Dor* 2007;15:6–65.
- Baliki MN, Geha PY, Jabakhanji R, Harden N, Schnitzer TJ, Apkarian AV. A preliminary fMRI study of analgesic treatment in chronic back pain and knee osteoarthritis. *Mol Pain* 2008;4:47.
- Baliki MN, Schnitzer TJ, Bauer WR, Apkarian AV. Brain morphological signatures for chronic pain. *PLoS One* 2011;6:e26010.
- Baliki MN, Petre B, Torbey S, Herrmann KM, Huang L, Schnitzer TJ, Fields HL, Apkarian AV. Corticostriatal functional connectivity predicts transition to chronic back pain. *Nat Neurosci* 2012;15:1117–19.
- Balke B. A simple field test for the assessment of physical fitness. *Rep 63-6. Rep Civ Aeromed Res Inst US* 1963;1–8. Available at: https://www.faa.gov/data_research/research/med_humanfacs/oamtechreports/1960s/media/am63-06.pdf
- Barroso J, Wakaizumi K, Reckziegel D, Pinto-Ramos J, Schnitzer T, Galhardo V, Apkarian AV. Prognostics for pain in osteoarthritis: do clinical measures predict pain after total joint replacement? *PLoS One* 2020;15:e0222370.
- Blikman T, Rienstra W, van Raay J, Dijkstra B, Bulstra SK, Stevens M, van den Akker-Scheek I. Neuropathic-like symptoms and the association with joint-specific function and quality of life in patients with hip and knee osteoarthritis. *PLoS One* 2018;13:e0199165.
- Bouhassira D, Attal N, Alchaar H, Boureau F, Brochet B, Bruxelle J, Cunin G, Fermanian J, Ginies P, Grun-Overdyking A, Jafari-Schluep H, Lanteri-Minet M, Laurent B, Mick G, Serrie A, Valade D, Vicaut E. Comparison of pain syndromes associated with nervous or somatic lesions and development of a new neuropathic pain diagnostic questionnaire (DN4). *PAIN* 2005;114:29–36.
- Cauda F, Palermo S, Costa T, Torta R, Duca S, Vercelli U, Geminiani G, Torta DM. Gray matter alterations in chronic pain: a network-oriented meta-analytic approach. *Neuroimage Clin* 2014;4:676–86.
- Centers for Disease Control and Prevention (CDC). Prevalence and most common causes of disability among adults—United States, 2005. *MMWR Morb Mortal Wkly Rep* 2009;58:421–6.

[15] Cohen J. Statistical power analysis for the behavioral sciences. 2nd ed. Hillsdale, NJ: Lawrence Erlbaum Assoc Publ. 2018, p. 558.

[16] Cottam WJ, Iwabuchi SJ, Drabek MM, Reckziegel D, Auer DP. 559 Altered connectivity of the right anterior insula drives the pain connectome changes in chronic knee osteoarthritis. *PAIN* 2018;159:929–38.

[17] Dabare C, Le Marshall K, Leung A, Page CJ, Choong PF, Lim KK. Differences in presentation, progression and rates of arthroplasty between hip and knee osteoarthritis: observations from an osteoarthritis cohort study—a clear role for conservative management. *Int J Rheum Dis* 2017;20:1350–60.

[18] Finan PH, Buenaver LF, Bounds SC, Hussain S, Park RJ, Haque UJ, Campbell CM, Haythornthwaite JA, Edwards RR, Smith MT. Discordance between pain and radiographic severity in knee osteoarthritis: findings from quantitative sensory testing of central sensitization. *Arthritis Rheum* 2013;65:363–72.

[19] Fingleton C, Smart K, Moloney N, Fullen BM, Doody C. Pain sensitization in people with knee osteoarthritis: a systematic review and meta-analysis. *Osteoarthritis Cartilage* 2015;23:1043–56.

[20] Friedman J, Hastie T, Tibshirani R. Regularization paths for generalized linear models via coordinate descent. *J Stat Softw* 2010;33:1–22.

[21] Goncalves RS, Cabri J, Pinheiro JP, Ferreira PL. Cross-cultural adaptation and validation of the Portuguese version of the Knee injury and Osteoarthritis Outcome Score (KOOS). *Osteoarthritis Cartilage* 2009;17:1156–62.

[22] Gorgolewski KJ, Varoquaux G, Rivera G, Schwartz Y, Sochat VV, Ghosh SS, Maumet C, Nichols TE, Poline JB, Yarkoni T, Margulies DS, Poldrack RA. NeuroVault.org: a repository for sharing unthresholded statistical maps, parcellations, and atlases of the human brain. *Neuroimage* 2016;124:1242–4.

[23] Grömping U. Relative importance for linear regression in R: the package relaimpo. *J Stat Softw* 2006;17:1–27.

[24] Gustin SM, Peck CC, Wilcox SL, Nash PG, Murray GM, Henderson LA. Different pain, different brain: thalamic anatomy in neuropathic and non-neuropathic chronic pain syndromes. *J Neurosci* 2011;31:5956–64.

[25] Gwilym SE, Filippini N, Douaud G, Carr AJ, Tracey I. Thalamic atrophy associated with painful osteoarthritis of the hip is reversible after arthroplasty: a longitudinal voxel-based morphometric study. *Arthritis Rheum* 2010;62:2930–40.

[26] Hashmi JA, Baliki MN, Huang L, Baria AT, Torbey S, Hermann KM, Schnitzer TJ, Apkarian AV. Shape shifting pain: chronicification of back pain shifts brain representation from nociceptive to emotional circuits. *Brain* 2013;136:2751–68.

[27] Hawker GA. Experiencing painful osteoarthritis: what have we learned from listening? *Curr Opin Rheumatol* 2009;21:507–12.

[28] Hochman JR, Davis AM, Elkayam J, Gagliese L, Hawker GA. Neuropathic pain symptoms on the modified painDETECT correlate with signs of central sensitization in knee osteoarthritis. *Osteoarthritis Cartilage* 2013;21:1236–42.

[29] IASP. IASP Terminology 2018 [definitions of pain terminology]. 2018. Available at: <http://www.iasp-pain.org/Education/Content.aspx?Itemnumber=1698>. Accessed September 2019.

[30] Jenkinson M, Bannister P, Brady M, Smith S. Improved optimization for the robust and accurate linear registration and motion correction of brain images. *Neuroimage* 2002;17:825–41.

[31] Jenkinson M, Beckmann CF, Behrens TE, Woolrich MW, Smith SM. Fsl. *Neuroimage* 2012;62:782–90.

[32] Kellgren JH, Lawrence JS. Radiological assessment of osteo-arthrosis. *Ann Rheum Dis* 1957;16:494–502.

[33] Kennard RW, Stone LA. Computer aided design of experiments. *Technometrics* 1969;11:137–48.

[34] Lewis GN, Parker RS, Sharma S, Rice DA, McNair PJ. Structural brain alterations before and after total knee arthroplasty: a longitudinal assessment. *Pain Med* 2018;19:2166–76.

[35] Lindeman RH, Merenda PF, Gold RZ. Introduction to bivariate and multivariate analysis. Glenview: Scott Foresman, 1980. p. 119.

[36] Maeda Y, Kettner N, Sheehan J, Kim J, Cina S, Malatesta C, Gerber J, McManus C, Mezzacappa P, Morse LR, Audette J, Napadow V. Altered brain morphometry in carpal tunnel syndrome is associated with median nerve pathology. *Neuroimage Clin* 2013;2:313–19.

[37] Malfait AM, Schnitzer TJ. Towards a mechanism-based approach to pain management in osteoarthritis. *Nat Rev Rheumatol* 2013;9:654–64.

[38] Mansour A, Baria AT, Tetreault P, Vachon-Presseau E, Chang PC, Huang L, Apkarian AV, Baliki MN. Global disruption of degree rank order: a hallmark of chronic pain. *Sci Rep* 2016;6:34853.

[39] Mao CP, Bai ZL, Zhang XN, Zhang QJ, Zhang L. Abnormal subcortical brain morphology in patients with knee osteoarthritis: a cross-sectional study. *Front Aging Neurosci* 2016;8:3.

[40] Mechelli A, Price CF. Voxel-based morphometry of the human brain: methods and applications. *Curr Med Imaging Rev* 2005;1:9.

[41] Murphy SL, Phillips K, Williams DA, Clauw DJ. The role of the central nervous system in osteoarthritis pain and implications for rehabilitation. *Curr Rheumatol Rep* 2012;14:576–82.

[42] Murray CJ, Vos T, Lozano R, Naghavi M, Flaxman AD, Michaud C, Ezzati M, Shibuya K, Salomon JA, Abdalla S, Aboyans V, Abraham J, Ackerman I, Aggarwal R, Ahn SY, Ali MK, Alvarado M, Anderson HR, Anderson LM, Andrews KG, Atkinson C, Baddour LM, Bahalim AN, Barker-Collo S, Barreiro LH, Bartels DH, Basanez MG, Baxter A, Bell ML, Benjamin EJ, Bennett D, Bernabe E, Bhalla K, Bhandari B, Bikbov B, Bin Abdulhak A, Birbeck G, Black JA, Blencowe H, Blore JD, Blyth F, Bolliger I, Bonaventure A, Boufous S, Bourne R, Boussinesq M, Braithwaite T, Brayne C, Bridgett L, Brooker S, Brooks P, Brugha TS, Bryan-Hancock C, Bucello C, Buchbinder R, Buckle G, Budke CM, Burch M, Burney P, Burstein R, Calabria B, Campbell B, Canter CE, Carabin H, Carapetis J, Carmona L, Celli C, Charlson F, Chen H, Cheng AT, Chou D, Chugh SS, Coffeng LE, Colan SD, Colquhoun S, Colson KE, Condon J, Connor MD, Cooper LT, Corriere M, Cortinovis M, de Vaccaro KC, Couser W, Cowie BC, Criqui MH, Cross M, Dabhadkar KC, Dahiya M, Dahodwala N, Damsons-Derry J, Danaei G, Davis A, De Leo D, Degenhardt L, Dellavalle R, Delossantos A, Denenberg J, Derrett S, Des Jarlais DC, Dharmaratne SD, Dherani M, Diaz-Torne C, Dolk H, Dorsey ER, Driscoll T, Duber H, Ebel B, Edmond K, Elbaz A, Ali SE, Erskine H, Erwin PJ, Espindola P, Ewoigbokhan SE, Farzadfar F, Feigin V, Felson DT, Ferrari A, Ferri CP, Fevre EM, Finucane MM, Flaxman S, Flood L, Foreman K, Forouzanfar MH, Fowkes FG, Fransen M, Freeman MK, Gabbe BJ, Gabriel SE, Gakidou E, Ganatra HA, Garcia B, Gaspari F, Gillum RF, Gmel G, Gonzalez- Medina D, Gosselin R, Grainger R, Grant B, Groeger J, Guillemin F, Gunnell D, Gupta R, Haagsma J, Hagan H, Halasa YA, Hall W, Haring D, Haro JM, Harrison JE, Havmoeller R, Hay RJ, Higashi H, Hill C, Hoen B, Hoffman H, Hotez PJ, Hoy D, Huang JJ, Ibeaneusi SE, Jacobsen KH, James SL, Jarvis D, Jasrasaria R, Jayaraman S, Johns N, Jonas JB, Karthikeyan G, Kassebaum N, Kawakami N, Keren A, Khoo JP, King CH, Knowlton LM, Kobusingye O, Koranteng A, Krishnamurthi R, Laden F, Laloo R, Laslett LL, Lathlean T, Leasher JL, Lee YY, Leigh J, Levinson D, Lim SS, Limb E, Lin JK, Lipnicki M, Lipshultz SE, Liu W, Loane M, Ohno SL, Lyons R, Mabwejano J, MacIntyre MF, Malekzadeh R, Mallinger L, Manivannan S, Marchemes W, March L, Margolis DJ, Marks GB, Marks R, Matsumori A, Matzopoulos R, Mayosi BM, McAnulty JH, McDermott MM, McGill N, McGrath J, Medina-Mora ME, Meltzer M, Mensah GA, Merriman TR, Meyer AC, Miglioli V, Miller M, Miller TR, Mitchell PB, Mock C, Mocumbi AO, Moffitt TE, Mokdad AA, Monasta L, Montico M, Moradi-Lakeh M, Moran A, Morawska L, Mori R, Murdoch ME, Mwaniki MK, Naidoo K, Nair MN, Naldi L, Narayan KM, Nelson PK, Nelson RG, Nevitt MC, Newton CR, Nolte S, Norman P, Norman R, O'Donnell M, O'Hanlon S, Olives C, Omer SB, Ortblad K, Osborne R, Ozgediz D, Page A, Pahari B, Pandian JD, Rivero AP, Patten SB, Pearce N, Padilla RP, Perez-Ruiz F, Perico N, Pesudovs K, Phillips D, Phillips MR, Pierce K, Pion S, Polanczyk GV, Polinder S, Pope CA, Popova S, Porrii E, Pourmalek F, Prince M, Pullan RL, Ramaiah KD, Ranganathan D, Razavi H, Regan M, Rehm JT, Rein DB, Remuzzi G, Richardson K, Rvara FP, Roberts T, Robinson C, De Leon FR, Ronfani L, Room R, Rosenfeld LC, Rushton L, Sacco RL, Saha S, Sampson U, Sanchez-Riera L, Sanman E, Schwebel DC, Scott JG, Segui-Gomez M, Shahraz S, Shepard DS, Shin H, Shivakoti R, Singh D, Singh GM, Singh JA, Singleton J, Sleet DA, Sliwa K, Smith E, Smith JL, Stapelberg NJ, Steer A, Steiner T, Stolk WA, Stovner LJ, Sudfeld C, Syed S, Tamburini G, Tavakkoli M, Taylor HR, Taylor JA, Taylor WJ, Thomas B, Thomson WM, Thurston GD, Tleyjeh IM, Tonelli M, Towbin JA, Truelson T, Tsilimbaris MK, Ubeda C, Undurraga EA, van der Werf MJ, van Os J, Vavilala MS, Venketasubramanian N, Wang M, Wang W, Watt K, Weatherall DJ, Weinstock MA, Weintraub R, Weisskopf MG, Weissman MM, White RA, Whiteford H, Wiebe N, Wiersma ST, Wilkinson JD, Williams HC, Williams SR, Witt E, Wolfe F, Woolf AD, Wulf S, Yeh PH, Zaidi AK, Zheng ZJ, Zonies D, Lopez AD, AlMazroa MA, Memish ZA. Disability-adjusted life years (DALYs) for 291 diseases and injuries in 21 regions, 1990–2010: a systematic analysis for the Global Burden of Disease Study 2010. *Lancet* 2012;380:2197–223.

[43] Neogi T. The epidemiology and impact of pain in osteoarthritis. *Osteoarthritis Cartilage* 2013;21:1145–53.

[44] Nilssdotter AK, Lohmander LS, Klassbo M, Roos EM. Hip disability and osteoarthritis outcome score (HOOS)—validity and responsiveness in total hip replacement. *BMC Musculoskeletal Disorders* 2003;4:10.

[45] Pais-Ribeiro J, Silva I, Ferreira T, Martins A, Meneses R, Baltar M. Validation study of a Portuguese version of the Hospital Anxiety and Depression Scale. *Psychol Health Med* 2007;12:225–35; quiz 235–7.

[46] Parks EL, Geha PY, Baliki MN, Katz J, Schnitzer TJ, Apkarian AV. Brain activity for chronic knee osteoarthritis: dissociating evoked pain from spontaneous pain. *Eur J Pain* 2011;15:843.e1–14.

[47] Podsiadlo D, Richardson S. The timed “Up & Go”: a test of basic functional mobility for frail elderly persons. *J Am Geriatr Soc* 1991;39: 142–8.

[48] Poldrack R. Can cognitive processes be inferred from neuroimaging data? *Trends Cogn Sci* 2006;10:59–63.

[49] Reckziegel D, Vachon-Presseau E, Petre B, Schnitzer TJ, Baliki MN, Apkarian AV. Deconstructing biomarkers for chronic pain: context- and hypothesis-dependent biomarker types in relation to chronic pain. *PAIN* 2019;160:S37–48.

[50] Rejeski WJ, Ettinger WH, Schumaker S, James P, Burns R, Elam JT. Assessing performance701 related disability in patients with knee osteoarthritis. *Osteoarthritis Cartilage* 1995;3:157–67.

[51] Rodriguez-Raecke R, Niemeier A, Ihle K, Ruether W, May A. Structural brain changes in chronic pain reflect probably neither damage nor atrophy. *PLoS One* 2013;8:e54475.

[52] Roos EM, Toksvig-Larsen S. Knee injury and Osteoarthritis 705 Outcome Score (KOOS)—validation and comparison to the WOMAC in total knee replacement. *Health Qual Life Outcomes* 2003;1:17.

[53] Shanahan CJ, Hodges PW, Wrigley TV, Bennell KL, Farrell MJ. Organisation of the motor cortex differs between people with and without knee osteoarthritis. *Arthritis Res Ther* 2015;17:164.

[54] Smith S, Nichols T. Threshold-free cluster enhancement: addressing problems of smoothing, threshold dependence and localisation in cluster inference. *NeuroImage* 2009;44:83–98.

[55] Smith SM, Zhang Y, Jenkinson M, Chen J, Matthews PM, Federico A, De Stefano N. Accurate, robust, and automated longitudinal and cross-sectional brain change analysis. *NeuroImage* 2002;17:479–89.

[56] Smith SM, Jenkinson M, Woolrich MW, Beckmann CF, Behrens TEJ, Johansen-Berg H, Bannister PR, De Luca M, Drobniak I, Filtney DE, Niazy RK, Saunders J, Vickers J, Zhang Y, De Stefano N, Brady JM, Matthews PM. Advances in functional and structural MR image analysis and implementation as FSL. *NeuroImage* 2004;23:S208–19.

[57] Somers TJ, Keefe FJ, Pells JJ, Dixon KE, Waters SJ, Riordan PA, Blumenthal JA, McKee DC, LaCaille L, Tucker JM, Schmitt D, Caldwell DS, Kraus VB, Sims EL, Shelby RA, Rice JR. Pain catastrophizing and pain-related fear in osteoarthritis patients: relationships to pain and disability. *J Pain Symptom Manage* 2009;37:863–72.

[58] Sullivan MJL, Bishop SR, Pivik J. The pain catastrophizing scale: development and validation. *Psychol Assess* 1995;7:524–32.

[59] Thakur M, Dickenson AH, Baron R. Osteoarthritis pain: nociceptive or neuropathic? *Nat Rev Rheumatol* 2014;10:374–80.

[60] Tibshirani R. Regression shrinkage and selection via the lasso. *J R Stat Soc Ser B Methodol* 1996;58:267–88.

[61] Tzourio-Mazoyer N, Landeau B, Papathanassiou D, Crivello F, Etard O, Delcroix N, Mazoyer B, Joliot M. Automated anatomical labeling of activations in SPM using a macroscopic anatomical parcellation of the MNI MRI single-subject brain. *NeuroImage* 2002;15:273–89.

[62] Vachon-Presseau E, Tétreault P, Petre B, Huang L, Berger SE, Torbey S, Baria AT, Mansour AR, Hashmi JA, Griffith JW, Comasco E, Schnitzer TJ, Baliki MN, Apkarian AV. Corticolimbic anatomical characteristics predetermine risk for chronic 739 pain. *Brain* 2016;139:1958–70.

[63] Wieland HA, Michaelis M, Kirschbaum BJ, Rudolphi KA. Osteoarthritis—an untreatable disease? *Nat Rev Drug Discov* 2005;4: 331–44.

[64] Winkler AM, Ridgway GR, Webster MA, Smith SM, Nichols TE. Permutation inference for the general linear model. *NeuroImage* 2014; 92:381–97.

[65] Yarkoni T, Poldrack RA, Nichols TE, Van Essen DC, Wager TD. Large-scale automated synthesis of human functional neuroimaging data. *Nat Methods* 2011;8:665–70.

[66] Zhang Y, Brady M, Smith S. Segmentation of brain MR images through a hidden Markov random field model and the expectation–maximization algorithm. *IEEE Trans Med Imaging* 2001;20:45–57.

[67] Zigmond AS, Snaith RP. The hospital anxiety and depression scale. *Acta Psychiatr Scand* 1983;67:361–70.